Thermal disordering of the Pt(110)-(1×2) surface

Michael A. Krzyzowski, Peter Zeppenfeld, Christoph Romainczyk, Rudolf David, and George Comsa
Institut für Grenzflächenforschung und Vakuumphysik, Forschungszentrum Jülich GmbH, D-52425 Jülich, Germany

Klaus E. Kuhnke and Klaus Kern
Institut de Physique Expérimentale, Ecole Polytechnique Fédérale de Lausanne, PH-Ecublens, CH-1015 Lausanne, Switzerland
(Received 16 May 1994; revised manuscript received 23 August 1994)

The temperature dependence of the structure of the clean, (1×2) reconstructed Pt(110) surface has been investigated by thermal-energy helium-atom scattering and low-energy electron diffraction. Two distinct phase transitions were observed: At about 1025 K a two-dimensional Isinglike transition from the well-ordered (1×2) missing-row reconstructed surface to a disordered but flat surface takes place, followed at about 1095 K by a Kosterlitz-Thouless transition into a rough phase. The measurements provide strong evidence for the phase in the intermediate-temperature regime being a flat phase like the *disordered flat phase* recently proposed by den Nijs. The precise microscopic structure of this intermediate phase, however, could not be quantified in detail.

I. INTRODUCTION

There is a fundamental interest of the surface science in phase transitions: On one hand, surfaces or adlayers constitute good testing grounds for theoretical models of phase transitions in two-dimensional (2D) systems. On the other hand, the analysis of the surface structure as a function of temperature provides insight into the energetics and thermodynamics of a surface. The Pt(110) surface is of particular interest for the second type of investigation since it allows for various phase transitions including deconstruction and roughening transitions. As platinum is a fcc crystal its (110) surface has the largest free energy of the low indexed surfaces. For this reason (111) facets (having the lowest surface free energy) can be built very easily on this (110) surface.[1] This may lead to a reconstruction or facetting of the crystal surface. Indeed, at room temperature the clean Pt(110) surface exhibits a (1×2) reconstruction which has been studied in detail using ion scattering,[2] low-energy electron diffraction (LEED),[3] x-ray diffraction,[4] and scanning tunneling microscopy.[5] Several reconstruction models have been discussed in the literature. The "missing-row" model [Fig. 1(a)], however, has been established by various measurements and calculations.[6–9] Owing to the open structure of the surface one expects clear manifestations of surface structure modifications with increasing surface temperature up to surface melting.[10] Indeed, a reversible order-disorder transition of the (1×2) reconstructed phase and a rough phase were observed well below the melting point.[11]

Besides the available experimental information, possible surface disordering mechanisms for the (1×2) reconstructed surface of a fcc crystal have also been investigated in detail by theory.[12] For the following discussion it is helpful to recall the crystallographic properties of the surface: Along the [001] direction of a (1×2) missing-row reconstructed fcc(110) surface the structure repeats every four distances $d \equiv a/\sqrt{2}$ (where $a = 2.77$ Å denotes the bulk nearest-neighbor distance for platinum). Note that d, rather than $2d$, is the smallest distance between atomic rows along the [001] direction if the second and deeper layers are considered [see Fig. 1(a)]. It is often convenient to express disorder of the atomic arrangement in terms of a phase difference, the periodic distance $4d$ of the perfectly ordered (1×2) phase corresponding to a phase difference of 2π. Four nonequivalent sublattices of the reconstructed surface can be defined, so that it is possible to generate three different "elementary displacements" characterized by phase differences: $n\pi/2$, with $n = 1$, 2, and 3.[13] These displacements can be divided into two classes. Defects introducing a phase difference of $\pi, 3\pi, \ldots$ [Figs. 1(b) and 1(c)] do not change the mean surface level, and constitute conventional antiphase domain boundaries within a (1×2) reconstructed single terrace. The other class of defects lead to a phase difference of $\pi/2$ or $3\pi/2$ and are necessarily connected with a surface step [Figs. 1(d) and 1(e)]. Across the step the terrace level changes by h, where $h = a/2$ is the interlayer spacing. All other surface defects along this direction can be generated by a combination of these elementary displacements.

The defects described above destroy the long-range (1×2) order of the reconstructed surface. If only defects of the first class are involved (phase difference $\pi, 3\pi, \ldots$) the surface, ideally, remains perfectly planar. If defects introducing surface steps are involved, the surface will exhibit multiple terraces. Depending on the succession of these defects on the surface, two fundamentally different situations can arise: Either the surface becomes rough, i.e., the height-height correlation along the surface diverges with lateral separation or the surface remains essentially flat, forming alternating up and down terraces. In the latter case, the structure is called a "disordered flat (DOF) phase."[14] Since defects introducing steps on the surface seem to cost a relatively low extra free energy and

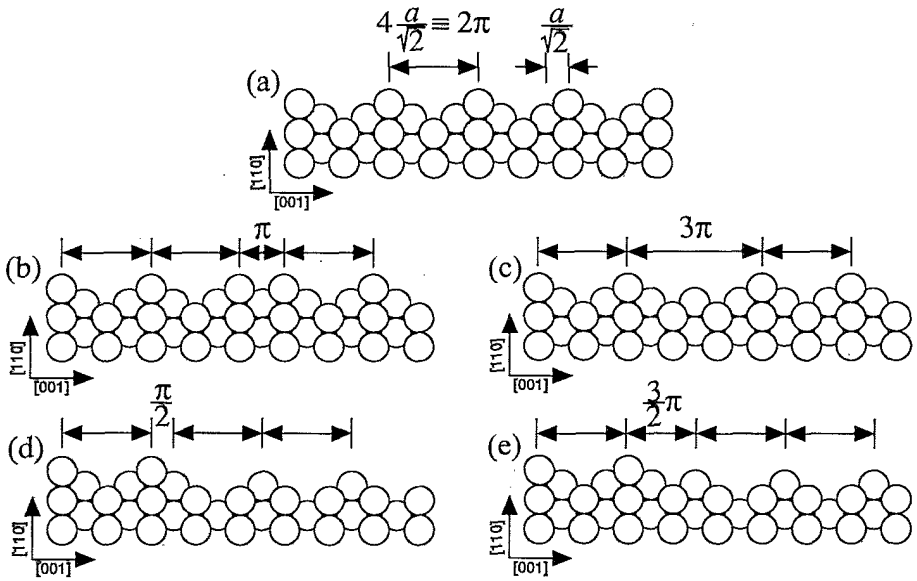

FIG. 1. Side view of the (1×2) reconstructed fcc(110) surface. The structure of the reconstructed surface has a periodicity of $4d$ along the [001] direction where $d \equiv a/\sqrt{2}$ and is the nearest-neighbor distance. A phase difference of 2π is assigned to the separation between two equivalent lattice sites on the unperturbed surface ($4d$) (a). Two different classes of elementary surface defects can be distinguished: (i) antiphase domain walls as shown in (b) and (c), introducing a phase difference of π or 3π. Here the mean surface level does not change, (ii) steps, as shown in (d) and (e), introducing a phase difference of $\pi/2$ and $3\pi/2$, respectively. Here the mean surface level changes by an interlayer spacing.

can, therefore, be created rather easily on the surface,[13] it is interesting to characterize the two different order-disorder transitions and to ask how they can be distinguished experimentally. We will start by briefly summarizing the theoretical results obtained for the transition from a (1×2) flat phase into a rough phase and a disordered flat phase, respectively.

The Pt(110) surface, ideally, is a flat surface and, indeed, a phase transition of interest here would be a surface roughening transition proceeded by the generation of steps through defects as depicted in Figs. 1(d) and 1(e). In general, the roughening temperature is defined as the temperature at which the free energy for generating a step vanishes.[15] At this point, new steps are created spontaneously on the surface[16] and new terraces are generated. Chui and Weeks[17] have shown that the surface roughening transition is of the Kosterlitz-Thouless type.[18] It is a very smooth (infinite-order) transition. The appropriate quantity that characterizes the rough surface is the height-height correlation function. According to theory this function diverges logarithmically for temperatures above the roughening temperature T_R,[19]

$$\langle [h(r_0+r)-h(r_0)]^2 \rangle = \frac{1}{2\pi} A(T) a_\perp^2 \ln \left[\frac{r^2}{a_\parallel^2} \right] . \qquad (1)$$

$A(T)$ increases monotonously with temperature. At the roughening temperature T_R, $A(T_R)=2/\pi$. $a_\perp$ and $a_\parallel$ are the lattice parameters perpendicular and parallel to the surface, respectively. Due to the logarithmic dependence on r the divergence is rather weak. This becomes more obvious in the "snapshots" of computer simulations of thermal roughening based, for instance, on the solid-on-solid (SOS) model.[20]

Besides a roughening transition, an ordered flat phase can also turn into a DOF phase. A detailed discussion of the DOF phase, which was introduced by den Nijs and Rommelse, can be found in Refs. 14 and 21–23. As mentioned previously there are two classes of elementary surface defects: domain walls and steps. To what extent each of them will actually contribute to the DOF phase depends on the ratio $R = E_w/E_s$ between the free energy E_w needed to create a domain wall and E_s needed to create a step. Both types of defects introduce a local disturbance of the surface order. In the case of a (1×2) reconstructed fcc(110) surface the lateral periodicity of $4d$ is destroyed leading to a "deconstruction." Even though steps are generated, these steps are correlated in such a way that the height correlation function in the DOF phase does not diverge. This is possible if a strong interaction between steps exists in such a way that an arrangement of successive up and down steps (i.e., steps with opposite sign) is favored with respect to an arrangement with neighboring steps having the same sign. In such a situation a surface with a sequence of alternating up and down steps is energetically favored with respect to a system with steps of the same orientation. As a consequence, the surface will remain essentially flat with only two exposed terrace levels. This behavior can be described in the framework of the restricted SOS model which takes into account nearest-neighbor as well as next-nearest-neighbor interactions.

Since steps introduce a lateral phase shift on the (1×2) reconstructed fcc(110) surface and hence destroy the (1×2) order, a roughening transition on such a surface is necessarily connected with a deconstruction, too—in contrast to the reconstructed sc(100) surface.[24] This implies that on a fcc(110)-(1×2) surface no roughening can occur *before* the surface is deconstructed. Yet, two different scenarios of the order-disorder transition of the fcc(110)-(1×2) surface are still possible: (1) the surface first deconstructs and then roughens at some higher temperature and (2) the disordering transition is a combination of a simultaneous deconstruction and roughening. For $R<2$ Campuzano, Jennings, and Willis[25] have calculated that the combined transition is an Ising transition. den Nijs has calculated that, also for $R>2$, the transition would be of the Ising type. Hence, in the case of a combined deconstruction and roughening the *visible* transition should be Ising-like. If, however, the deconstruction is followed by a roughening we first expect an Ising transition (from the reconstructed to the deconstructed phase) followed at higher temperature by a Kosterlitz-Thouless transition (from the deconstructed flat to the rough phase).

The Pt(110)-(1×2) surface phase transition has already been studied experimentally by Robinson and co-workers[11] using x-ray diffraction and Korte and Meyer-Ehmsen[26] using reflection high-energy electron diffraction (RHEED). Robinson and co-workers have reported an increase of the step density connected with a disordering of the (1×2) structure conforming to an Ising transition at a critical temperature of about 1080 K. Korte and Meyer-Ehmsen also find a 2D Ising-like transition (with a critical temperature $T_c=855$ K) which they attribute to a deconstruction of the (1×2) phase. In addition, they claim the onset of surface roughening to occur at about 20–50 K *above* T_c. This would suggest separate deconstruction and roughening transitions. However, the critical temperatures associated with the two transitions are much lower than the roughening temperature reported previously for this system.

A He-scattering investigation of the Au(110)-(1×2) surface [which exhibits the same structure as Pt(110)-(1×2)] by Sprösser, Salanon, and Lapujoulade[27] has shown that in this case there exist two separate transitions: a deconstruction transition at $T_c=650$ K and a transition related to the onset of step proliferation at $T_R=690$ K.

We note that there may exist still other structural transitions on the Pt(110)-(1×2) surface such as the generation of the particular defect structure described in Ref. 28.

II. EXPERIMENT

The experiments were carried out in an ultrahigh vacuum He-scattering apparatus (base pressure in the 10^{-11} mbar range). The apparatus is equipped with a four-grid combined LEED-Auger optics, a nozzle generating a supersonic thermal He beam, and a He time-of-flight (TOF) spectrometer consisting of a pseudorandom chopper and an electron impact He detector with quadrupole mass analyzer. The energy of the He beam can be varied continuously from 17.8 meV up to above 100 meV by changing the nozzle temperature. The detection efficiency of the He detector is about 10^{-5},[29] the dead time of the detector was determined to $\tau_0\approx 0.7$ μs. In all the measurements reported below, the He intensity has been corrected for this dead time.

The overall scattering angle ϑ (i.e., the angle between the incident beam and the detector line) can be varied between 55° and 125° by rotating the TOF spectrometer in the horizontal scattering plane around the vertical polar axis of the sample. In addition, the sample can be rotated around its polar and azimuthal axes by means of a manipulator. Therefore, diffraction spectra can be taken either by "detector scans" or "manipulator scans." In the usual scattering geometry the incident beam, the scattered beam, and the surface normal lie in the same plane. In this case the He wave-vector transfer parallel to the surface Q can be written as $Q=k_i[\sin\vartheta_f-\sin\vartheta_i]$, where k_i is the wave vector of the incident He beam and ϑ_i and ϑ_f are the incident and outgoing angles, respectively, measured against the surface normal. Bragg peaks are expected if Q coincides with a reciprocal surface lattice distance (for instance, $Q=1.85$ Å^{-1} for the (0,1) peak and $Q=0.93$ Å^{-1} for the half-order diffraction peak $(0,\frac{1}{2})$ along the [001] direction of the Pt(110) surface). All peak heights and diffraction profiles reported in this paper are based on time integrated intensities.

The Pt(110) crystal was cleaned *in situ* by repeated cycles of heating in an oxygen atmosphere ($1-5\times10^{-6}$ mbar at $T=750$ K), followed by flashing to $T=1250$ K, and sputtering with 0.7 keV argon ions at $T=700$ K followed by annealing at around 1200 K. During the final cooling the crystal was held at 900 K for several minutes allowing the development of a well-ordered (1×2) reconstruction.

III. RESULTS

A. The Pt(110)-(1×2) reconstructed surface

After sputtering and careful annealing of the Pt(110) crystal a well ordered (1×2) reconstructed surface is obtained at room temperature. This is evidenced by the sharp half-order diffraction peaks along the [001] direction in the He-diffraction scans (Fig. 2). Due to preexisting steps on the surface, the peak profile of the He-(0,0)-diffraction peak (specular peak) depends on the scattering conditions: If the scattering conditions are chosen such that terraces separated by a monoatomic step of height h scatter in phase (i.e., if $k_i[\cos(\vartheta_i)+\cos(\vartheta_f)]h=n2\pi$, with n an integer) the peak profile can be described quite well by a single Gaussian curve [Fig. 3(a)]. This curve has a full width at half maximum (FWHM) of $\Delta Q=0.012$ Å^{-1} and corresponds to the instrument function.[29] Under antiphase conditions (i.e., if $k_i[\cos(\vartheta_i)+\cos(\vartheta_f)]h=(n+\frac{1}{2})2\pi$, with n an integer) the specular diffraction peak develops a markedly broadened foot, reflecting the presence and distribution of terraces separated by atomic steps [Fig. 3(b)]. By varying the

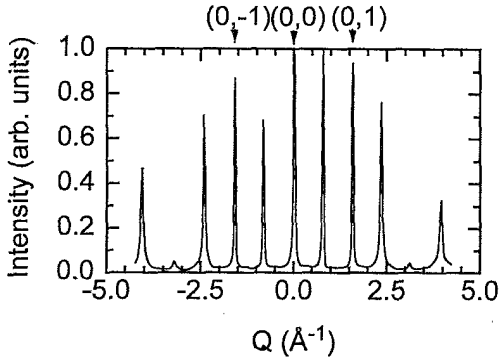

FIG. 2. Helium diffraction spectrum of the clean Pt(110) surface taken along the [001] direction (He beam energy: $E_{He}=17.8$ meV, surface temperature $T=300$ K).

scattering conditions (e.g., by changing the total scattering angle) while monitoring the diffraction peak height and width the step height h can be extracted. As a result, we obtain $h=1.40\pm0.01$ Å, in good agreement with the expected crystallographic value $h=a/2=1.39$ Å. The antiphase profile [Fig. 3(b)] is well approximated by a sum of a Gaussian (with the same FWHM as for the in-phase diffraction peak) and a Lorentzian curve convoluted with the same Gaussian instrument function. Hence, the Gaussian part of the antiphase diffraction peak profile corresponds to the Bragg peak due to the scattering from extended terraces broadened only by the instrument function, while the Lorentzian part contains the contribution from smaller terraces. From the FWHM of the Lorentzian curve ΔQ, a characteristic terrace width D can be extracted according to $\Delta Q\approx 2\pi/D$. In the present case we obtain $D\approx 130$ Å for the average size of the small terraces.

B. Debye-Waller attenuation of the Pt(110)-(1×2) diffraction intensities

In order to obtain information on the evolution of the surface structure with temperature we have investigated as a first step the height of the Pt(110)-(1×2) diffraction peaks as a function of surface temperature. The peak height of the diffraction peak intensities should decay with temperature just because of the increasing contribution of thermally excited vibrations of the surface atoms. This well-known Debye-Waller effect does not change the peak profile. Quantitatively, the effect on the diffraction peak height is given by[30]

$$I(T)=I_0 e^{-2W(T)} . \tag{2}$$

Equation (2) should be regarded as a definition of a Debye-Waller behavior. A proper derivation of W does exist for neutron and x-ray scattering only, and is based on the Born approximation. For He scattering from surfaces, calculations of the Debye-Waller factor do, however, suggest that a similar relation as for neutron and x-ray scattering should also hold for He atoms,[31–33] namely

$$2W=\langle(\mathbf{q}\cdot\mathbf{u}_{\text{eff}})^2\rangle . \tag{3}$$

Here $\mathbf{u}_{\text{eff}}$ is the effective thermal displacement of the surface atoms out of their equilibrium position, $\langle\ \rangle$ denotes the thermal averaging and $\mathbf{q}$ the scattering wave-vector transfer. More precisely, $\mathbf{u}_{\text{eff}}$ describes the local thermal displacement of the He-surface interaction potential. As a consequence, $\mathbf{u}_{\text{eff}}$ is correlated with the position of the lattice atoms via the electron-density distribution above

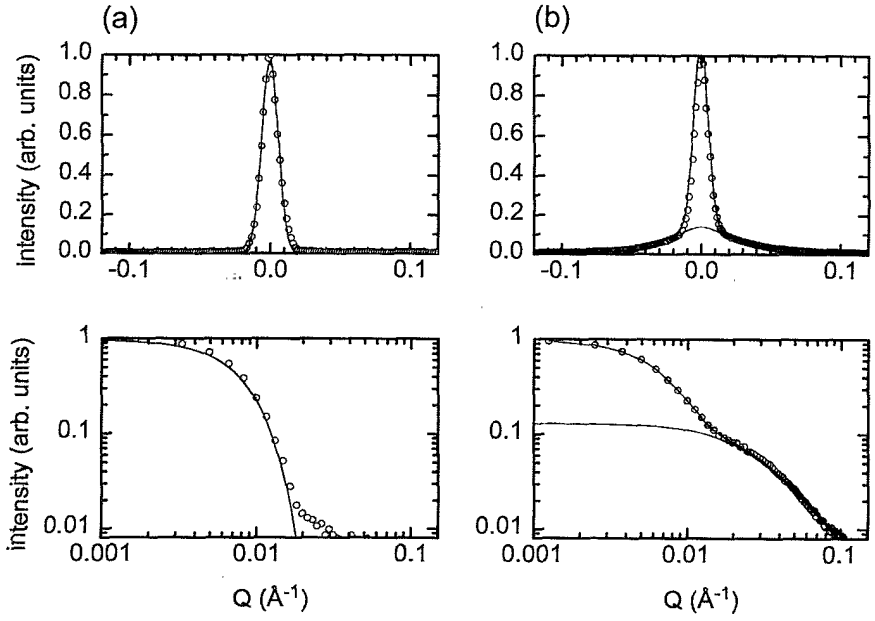

FIG. 3. He-diffraction peak profiles of the specular peak for in-phase (a) and antiphase scattering conditions (b). The upper panels provide a linear scale, while the lower panels are double-logarithmic representations of the same profiles. The solid lines are fits to a single Gaussian instrument function (a) and the sum of a Gaussian and a Lorentzian convoluted with the instrument function (b). The scattering conditions were $\vartheta=78.9°$ for the in-phase and $\vartheta=108.6°$ for the antiphase condition, He-beam energy $E_{He}=17.8$ meV; the surface temperature was $T=300$ K.

the surface from which the He atoms are scattered.[34] It should be noted that the resulting electron-density distribution depends on the position of several neighboring atoms, especially for metals. This is a major difference with respect to the physics of neutron or x-ray scattering. This was pointed out by Hoinkes, Nahr, and Wilsch[35] and Armand and Manson[36] and is often referred to as the *Armand effect.* Another important aspect is the fact that the well depth of the He-surface potential D has to be taken into account to determine the perpendicular wave-vector transfer *(Beeby correction).* With $\mathbf{q}\equiv(Q,q_\perp)$ we get

$$Q=(k_{i\parallel}-k_{f\parallel})\,, \tag{4a}$$

$$q_\perp=\left[k_{i\perp}^2-\frac{2m}{\hbar^2}D\right]^{1/2}+\left[k_{f\perp}^2-\frac{2m}{\hbar^2}D\right]^{1/2}. \tag{4b}$$

The well depth D of the He-Pt(110) interaction potential was obtained to be $D=-8.17$ meV.[37] $k_{i\parallel}$, $k_{f\parallel}$ and $k_{i\perp}$, $k_{f\perp}$ are the parallel and orthogonal components of the momentum of the incoming and outgoing particle, respectively, and m is the mass of the helium atom. Solving (3) for parallel and orthogonal terms we obtain

$$\begin{aligned}2W(T)&=\langle(q_\perp u_{\rm eff}+QU_{\rm eff})^2\rangle\\&=q_\perp^2\langle u_{\rm eff}^2\rangle+\sum_\alpha\left[2q_\perp Q_\alpha\langle u_{\rm eff}U_{{\rm eff},\alpha}\rangle\right.\\&\qquad\left.+Q_\alpha^2\langle U_{{\rm eff},\alpha}^2\rangle\right],\end{aligned} \tag{5}$$

with $\alpha=x,y$ and $u_{\rm eff}$, $U_{\rm eff}$ the effective displacements of the surface atoms out of their equilibrium positions perpendicular and parallel to the surface, respectively. For specular scattering ($Q=0$) (5) reduces to

$$2W_{\rm sp}(T)=q_\perp^2\langle u_{\rm eff}^2\rangle\,. \tag{6}$$

For usual scattering geometry it can be shown that the sum in (5) is small compared to the first term, even for the higher-order diffraction peaks,[38] so that (6) can be used as a good approximation for all diffraction peaks considered here. $\langle u_{\rm eff}^2\rangle$ is the temperature-dependent part of the Debye-Waller factor. To a first approximation the dependence of $\langle u_{\rm eff}^2\rangle$ on the surface temperature is the same as the dependence of the displacement of the surface atoms themselves. For a harmonic lattice the mean-square displacement is proportional to the surface temperature T.[39] We finally obtain an expression that is similar to the one known for the bulk crystal[40]

$$\langle u_{\rm eff}^2\rangle=\frac{3\hbar^2}{mk_B}\frac{T}{\Theta_{D,\rm eff}^2}\,. \tag{7}$$

Note, however, that the Debye temperature of the solid Θ_D has to be replaced by an effective surface Debye temperature $\Theta_{D,\rm eff}$.

In Fig. 4 the measured peak heights of the (0,0) and (0,1) diffraction peaks of the Pt(110) surface for in-phase and antiphase conditions are shown. In the lower-temperature range the intensity of the peaks decreases exponentially as expected for a pure Debye-Waller effect. A peak profile analysis showed no change in the profile within this temperature range. According to Eqs. (2)–(7), we have extracted effective Debye temperatures for the different peaks and scattering conditions. As a re-

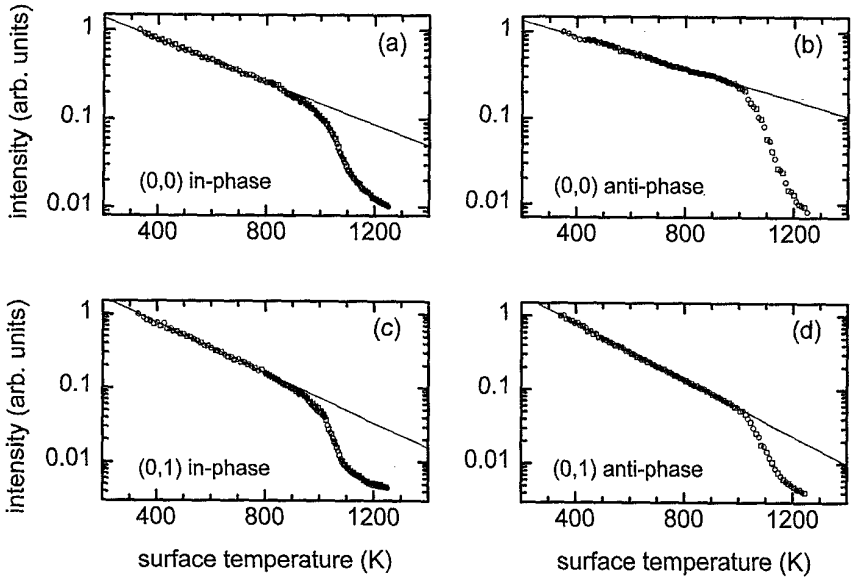

FIG. 4. Logarithm of the peak height of the integral-order diffraction peaks as a function of surface temperature: The diagrams show the peak height of the specular diffraction peak (0,0) for in-phase (a) ($E_{\rm He}=17.8$ meV, $\vartheta_i=38.96°$) and antiphase conditions (b) ($E_{\rm He}=17.8$ meV, $\vartheta_i=54.32°$), as well as the first-order diffraction peak (0,1) for in-phase (c) ($E_{\rm He}=31.2$ meV, $\vartheta_i=34.2°$) and antiphase conditions (d) ($E_{\rm He}=43.1$ meV, $\vartheta_i=34.2°$). Circles correspond to measurements taken while increasing the temperature and squares while decreasing the temperature. The straight lines indicate a pure Debye-Waller behavior. The effective Debye temperatures obtained from the fits in the lower temperature range are (a) $\Theta_{D,\rm eff}=198$ K, (b) $\Theta_{D,\rm eff}=196$ K, (c) $\Theta_{D,\rm eff}=197$ K, and (d) $\Theta_{D,\rm eff}=200$ K, resulting in a mean effective Debye temperature $\Theta_{D,\rm eff}=198\pm2$ K.

sult, we find $\Theta_{D,\text{eff}}=198\pm2$ K.[41] This value should be compared to the measured effective Debye temperature of the Pt(111) surface ($\Theta_{D,\text{eff}}=231\pm2$ K).[42] The two values are rather similar and, as expected, the surface with the more open structure, the (110) surface, has a lower effective Debye temperature than the more densely packed Pt(111) surface.

An inspection of the curves in Fig. 4 clearly shows that a deviation from the simple Debye-Waller behavior occurs at around 1000 K for scattering at antiphase conditions and somewhat lower temperatures for in-phase scattering conditions. The precise origin of the earlier, more gradual deviation for the in-phase intensity curves is not known. We have, however, observed an even smoother behavior than the one depicted in Figs. 4(b) and 4(d) during our first measurements on this surface. After repeated careful preparation, the in-phase curves eventually approached the more abrupt shape characteristic for the antiphase curves. The difference between the two curves could, therefore, be possibly related to residual steps or impurities on the surface. Note that the intensity curves in Fig. 4 recorded during increasing and decreasing the temperature are identical. Thus, the corresponding thermal anomaly of the Pt(110) surface is completely reversible.

A deviation from the simple Debye-Waller behavior above a given temperature has been observed previously on several other surfaces as well. In some cases this was attributed to an increase of the surface anharmonicity, leading to an enhanced vibration amplitude for the surface atoms.[43,44] Besides, structural disorder, such as thermally generated steps, adatom-vacancy pairs, or (segregated) impurities, can be responsible for a sudden decrease in the diffraction intensities.[45]

To distinguish between the different possibilities and to unravel the origin of the anomaly in the thermal attenuation of the diffraction peaks, it is indispensable to analyze the entire peak profiles of the various diffraction peaks. This analysis is described in the following two sections.

C. Surface deconstruction

The information on the order parameter connected with the (1×2) periodicity of the reconstructed surface can be extracted from the change of the peak height and the peak profile of the half-order diffraction peaks. The corresponding peak profiles have been measured at different surface temperatures to investigate the thermal stability of the reconstruction. One problem in the analysis of the half-order diffraction peak is the knowledge of the correct in-phase and antiphase scattering conditions. They depend on the nature and on the sign (i.e., up or down) of surface steps separating neighboring terraces. The two types of steps [Fig. 1(d) and 1(e)] introduce a phase shift that differs by π. If both of them have the same sign, in-phase scattering across the first type of steps corresponds to antiphase scattering for the second type of steps and *vice versa*. In the case of *steps of the same type*, but with opposite sign, the behavior is similar: if the up step is in in-phase the down step of the same type is in antiphase and *vice versa*. According to Fenter and Lu[46] the presence of steps can lead to a periodic change in the position of the half-order peak as the scattering condition (and hence the normal momentum transfer) is varied. The amplitude of this peak shift depends on the difference between the number of the two types of steps. In the presence of a single type of step the width of the half-order peaks does not depend on the normal momentum transfer.[46] However, a variation of the FWHM is expected if both types of steps occur and if the majority of the type of up steps differs from that of the down steps or if at the surface a significant number of double height steps exist.[27] By varying the scattering geometry as well as the energy of the incident He beam for the $(0,\frac{1}{2})$ and $(0,-\frac{1}{2})$ diffraction peaks no significant changing in the peak position nor in the peak profile could be detected. Based on the FWHM of the half-order peaks of about 0.02 Å^{-1} it could be concluded that the shift between in-phase and antiphase is smaller than 0.01 Å^{-1}. Therefore, the excess density of the majority steps, i.e., the difference between the two kinds of steps, is smaller than 0.06 steps per unit cell.[46] This value leads to an upper limit of the excess density of about 1/130 Å. Therefore, on the basis of these experiments, no clear answer can be given with respect to the energetically most favored type of step. It is also possible that both types of steps are present on the surface in similar concentration. In order not to overlook any possible effect on the change of the profile of the half-order diffraction peak with temperature, measurements were conducted for three different scattering conditions: the in-phase and antiphase conditions for either type and sign of step (corresponding to the antiphase and in-phase conditions for the other type and sign of step) and for an intermediate condition where the phase shift between neighboring terraces is $\pi/2$ for either type of step.

The results are shown in Fig. 5. For temperatures below 1000 K the intensity decrease of the half-order diffraction peaks follows a Debye-Waller behavior. The corresponding Debye temperatures are, as expected, consistent to those obtained from the integral-order diffraction peaks. Above 1040 K the peak heights of the half-order peaks decrease very rapidly. At around 1080 K the peaks can no longer be separated from the background. This behavior was also observed with LEED (see Fig. 6). The pictures show that the half-order diffraction spots disappear between 1000 and 1100 K. In this temperature range, the (1×2) reconstruction disorders completely, the surface deconstructs.

A more quantitative analysis of the He-diffraction intensities of the half-order peaks is presented in Fig. 7. After correction for the Debye-Waller factor the peak height dependence was fitted to the algebraic form characteristic for a second-order phase transition

$$I \propto (T_c - T)^{2\gamma} . \tag{8}$$

The critical exponent γ was determined to be $\gamma=0.13\pm0.02$,[47] in good agreement with the value $\gamma=0.11\pm0.01$ obtained by Robinson and co-workers[11] for Pt(110) and $\gamma=0.13\pm0.02$ for Au(110).[48] These values are close to the exponent of $\gamma=\frac{1}{8}$ expected for a

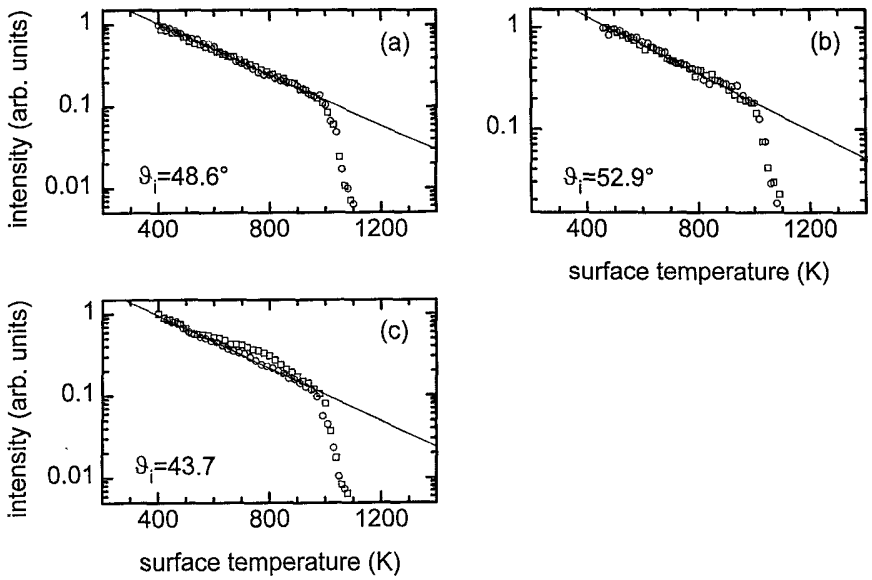

FIG. 5. Logarithm of the peak height of the half-order diffraction peaks as a function of surface temperature: (a) $E_{He}=31$ meV, $\vartheta_i=48.6°$: The scattering phase shift between neighboring terraces separated by either type of step is an odd multiple of $\pi/2$. (b) $E_{He}=31$ meV, $\vartheta_i=52.9°$: In-phase scattering for terraces separated by $\pi/2$ steps [Fig. 1(d)] and antiphase scattering for $3\pi/2$ steps [Fig. 1(e)]. (c) $E_{He}=31$ meV, $\vartheta_i=43.7°$: Antiphase scattering for terraces separated by $\pi/2$ steps and in-phase scattering for $3\pi/2$ steps. Circles indicate measurements taken while increasing the temperature and squares measurements while decreasing the temperature again. The straight lines correspond to an intensity decrease expected on the basis of the Debye-Waller effect. The effective Debye temperatures calculated from the fits in the lower temperature range are (a) $\Theta_{D,eff}=196$ K, (b) $\Theta_{D,eff}=197$ K, and (c) $\Theta_{D,eff}=202$ K.

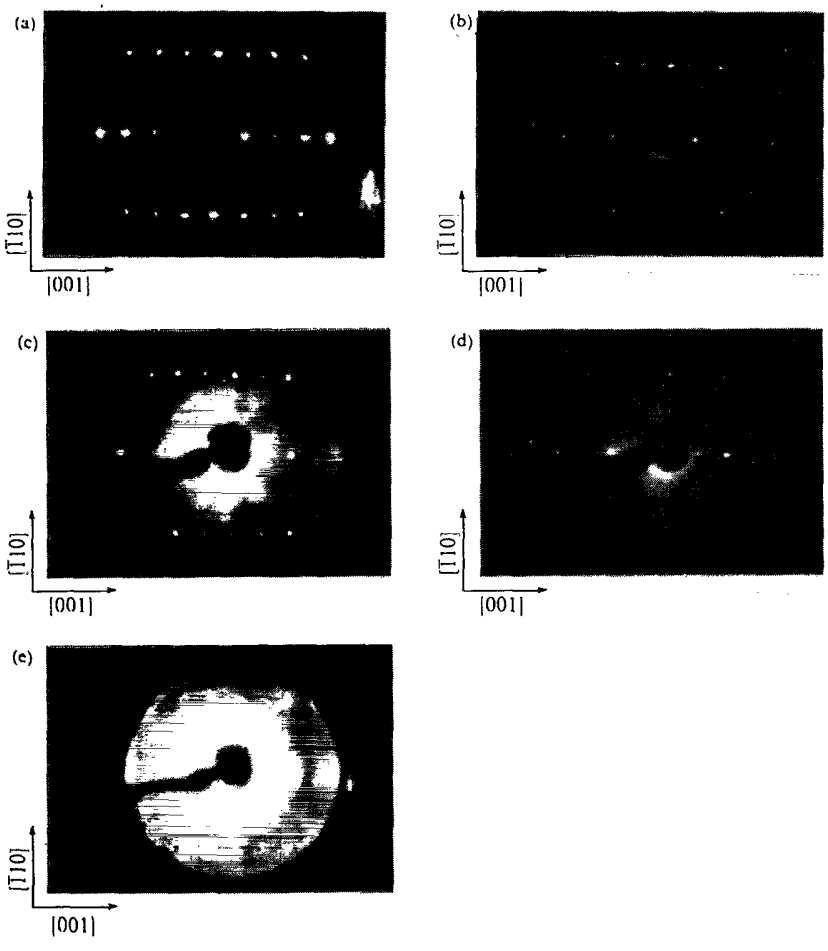

FIG. 6. LEED images taken from the Pt(110) surface for different surface temperatures (electron energy $E=136$ eV): (a) $T=300$ K, (b) $T=1000$ K, (c) $T=1040$ K, (d) $T=1080$ K, and (e) $T=1120$ K. At a temperature of 1040 K (c) the half-order diffraction peaks are broadened while the integral-order peaks are still sharp. These integral-order diffraction spots become diffuse only above $T=1080$ K (e).

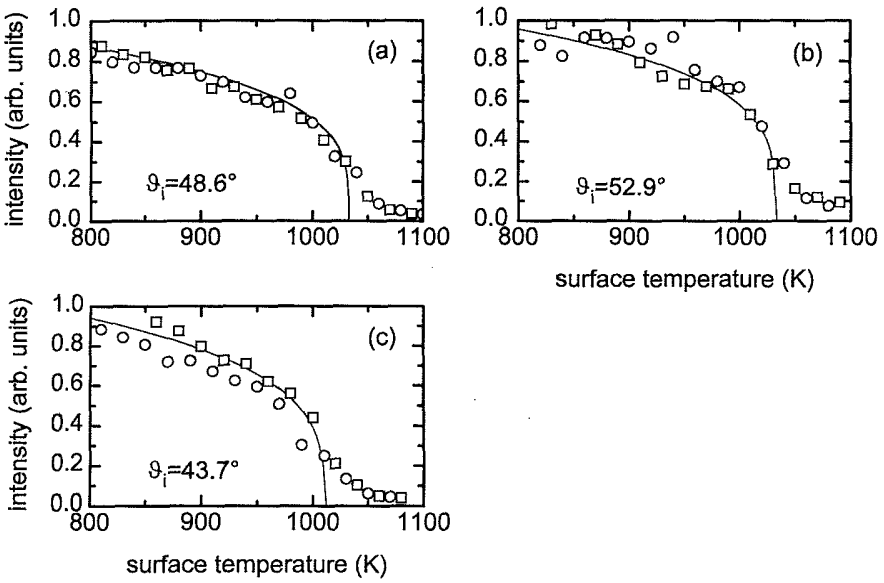

FIG. 7. Peak height of the half-order diffraction peak $(0,\frac{1}{2})$ in the temperature range close to the deconstruction transition. The intensities are corrected for the Debye-Waller factor. The solid lines are fits to Eq. (9) with (a) $T_c=1033$ K and $\gamma=0.13$, (b) $T_c=1032$ K and $\gamma=0.11$, (c) $T_c=1010$ K and $\gamma=0.14$. Other experimental parameters as in Fig. 5.

2D-Ising transition. Therefore, the deconstruction transition, indeed, appears to be of the Ising-type as predicted by den Nijs.[24] The critical temperature obtained from the fit in Fig. 7 is $T_c=1025\pm10$ K, in good agreement with the critical temperature obtained by Robinson and co-workers[11] but much higher than the value of 855 K reported in Ref. 26.

The analysis of the profiles of the half-order diffraction peaks (Fig. 8) shows that for all three scattering conditions the diffraction peak can be described by a sharp peak (broadened only by the instrument function) and by a broader part in the foot of the diffraction peak. The fact that no scattering conditions were found for which only a single sharp peak is observed (c.f. Fig. 3) can be explained by the fact that no clearly defined in-phase scattering condition exists, possibly due to the presence of both kinds of steps and/or domain walls. Furthermore, a preexisting in-plane disorder of the (1×2) periodicity, for instance due to local $(1\times n)$ reconstructions with $n=3,5,7,\ldots$, would also introduce constant phase shifts leading to a broadening of the half-order diffraction peaks.

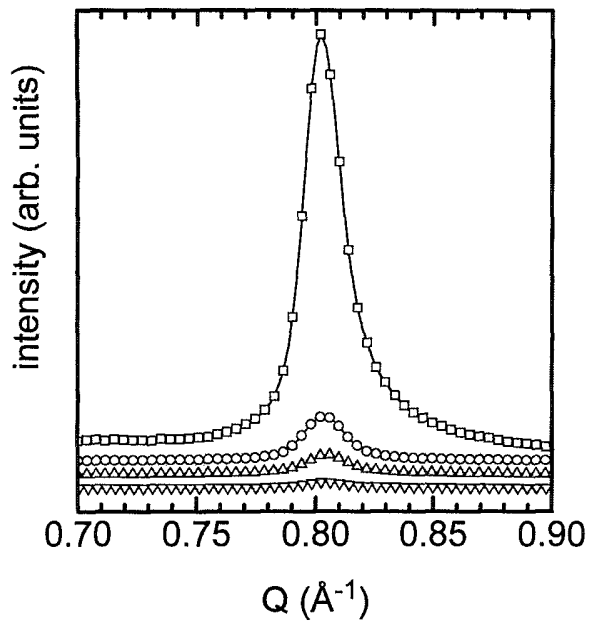

FIG. 8. Peak profiles of the $(0,\frac{1}{2})$ diffraction peak along the [001] direction ($E_{He}=31$ meV, $\vartheta_i=48.6°$) for different surface temperatures. From top to bottom: (□) $T=400$ K, (○) $T=1000$ K, (△) $T=1040$ K, and (▽) $T=1060$ K. For the other scattering conditions the profiles look very similar.

When increasing the surface temperature above 1000 K the intensity of the sharp component of the half-order diffraction peak decreases rapidly (see Fig. 5) while its width remains almost constant (Fig. 8). At temperatures just above the critical temperature the broad component of the diffraction peak becomes even broader and its relative condition to the total peak intensity increases rapidly. This is generally explained by the increase of the critical fluctuations close to the transition temperature. At still higher temperatures, the broad component of the half-order diffraction peak also loses its intensity and vanishes completely at around 1080 K.

Summarizing these results, we find strong evidence for an Ising-like deconstruction of the Pt(110)-(1×2) surface close to 1025 K. As we will show in the next section, the Pt(110) surface does not undergo a simultaneous roughening transition. Therefore, we believe that after the deconstruction the Pt(110) surface is in the DOF phase postulated by den Nijs.[24]

There remains the interesting question on the microscopic structure of this DOF phase. Comparing the intensity curves of the integer-order peaks (Fig. 4) with those of the half-order peaks (Fig. 7) in the temperature range between 1000 and 1100 K, it is obvious that the attenuation of the intensity of the half-order peaks is correlated with a similar strong attenuation of the intensity of the integer-order peaks above 1020 K. This can now be explained by the fact that during the deconstruction de-

fects are generated (see also Fig. 1), which scatter diffusely, thereby leading to an attenuation of both the in-phase and antiphase intensities of the integer-order peak. It seems, however, that for antiphase conditions the intensity of the integral-order peaks decreases more rapidly above 1020 K than for in-phase scattering conditions. This suggests that in addition to walls steps also [Figs. 1(d) and 1(e)] are generated which in addition to the diffuse scattering also lead to the appearance of new terraces. Indeed, this contribution would not be noticeable under in-phase conditions where the interference is constructive but it would lead to an enhanced intensity attenuation under antiphase conditions where the interference is destructive. The generation of steps should also affect the shape of the antiphase peak profiles of the integral-order diffraction peaks. From a quantitative analysis of the peak shapes the concentration and correlation between these steps can be studied. In particular, it is possible to conclude whether the generation of such steps leads to a rough phase and, if so, to determine the roughening temperature T_R. These questions are addressed in the following section.

D. Surface-roughening transition

The most prominent change in the peak profile of the integral-order peaks is the dramatic increase of the FWHM of the antiphase peaks above 1100 K (Fig. 9). The temperature-induced change of the profile, and hence the corresponding structural transition, are completely reversible. Since at this elevated temperature the half-order diffraction signatures in He scattering (Figs. 5, 7, and 8) and LEED (Fig. 6) have already disappeared we conclude that the phase transition takes place on the *deconstructed* surface. A broadening of the peaks at the antiphase condition indicates a decrease of the mean terrace width and a simultaneous increase of the step densities. In fact, a strong increase of the FWHM of the antiphase profile is expected for a surface-roughening transition.

The quantitative effect of a roughening transition on the He-diffraction peak profiles has been treated extensively in theory and experiment.[49–52] With a few assumptions the diffraction profiles of the rough phase $T > T_R$ can be described by a power-law line shape

$$I \propto Q^{-(2-\gamma)} , \tag{9}$$

where the roughening exponent γ depends on the surface temperature

$$\gamma = \frac{\pi}{2} A(T) f(\Phi) . \tag{10}$$

$f(\Phi)$ describes the dependence on the scattering conditions. Φ is the phase difference for scattering from terraces separated by a monoatomic step. The shape of $f(\Phi)$ varies according to the microscopic model.[52,53] However, for all models $f(\Phi)=0$ for a phase difference $\Phi=2n\pi$ (in-phase scattering) and $f(\Phi)=1$ for $\Phi=(2n+1)\pi$ (antiphase scattering), with n being an integer. The largest impact of the roughening transition on the peak profile is, therefore, expected for antiphase scattering conditions. $A(T)$ is the monotonous function defined in Eq. (1).

The peak profiles for the (0,0) specular diffraction peak at antiphase conditions are shown in Fig. 10 for different surface temperatures. With increasing temperature we observe a continuous change of the profile from a sum of a δ peak and a Lorentzian peak, both convoluted with the instrument function (see Fig. 3) to a profile described by Eq. (9) and convoluted with the instrument function. Consequently, the observed phase transition is consistent with a surface-roughening transition. At the roughening temperature T_R theory predicts that $A(T_R)=2/\pi$, corresponding to a power-law exponent $-[2-\gamma(T_R)]=-1$. A simple and precise way of deter-

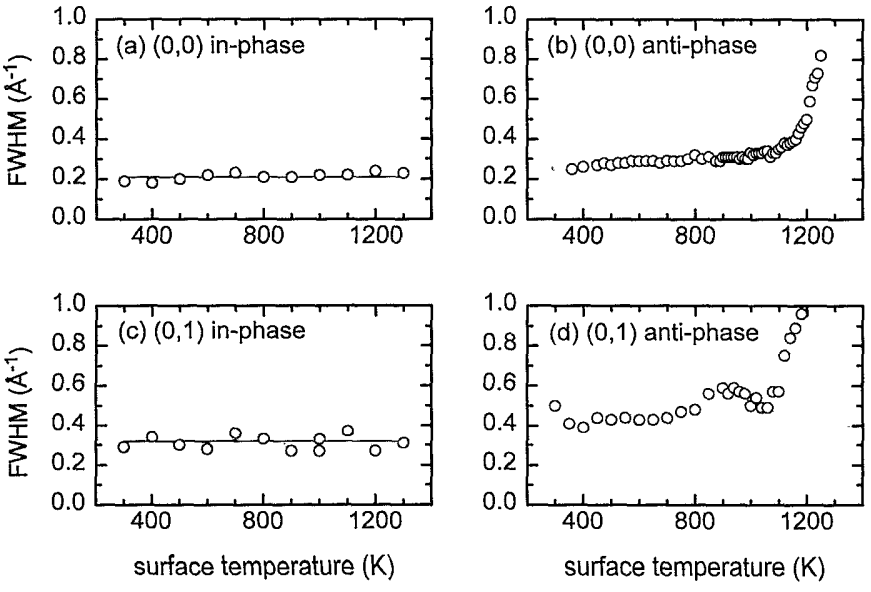

FIG. 9. FWHM of the integral-order diffraction peaks as a function of surface temperature. Specular intensity (0,0) for in-phase condition (a) and antiphase conditions (b); first-order diffraction peak (0,1) for in-phase (c) and antiphase scattering (d). The scattering conditions (He-beam energy and scattering angles) are the same as in Fig. 3.

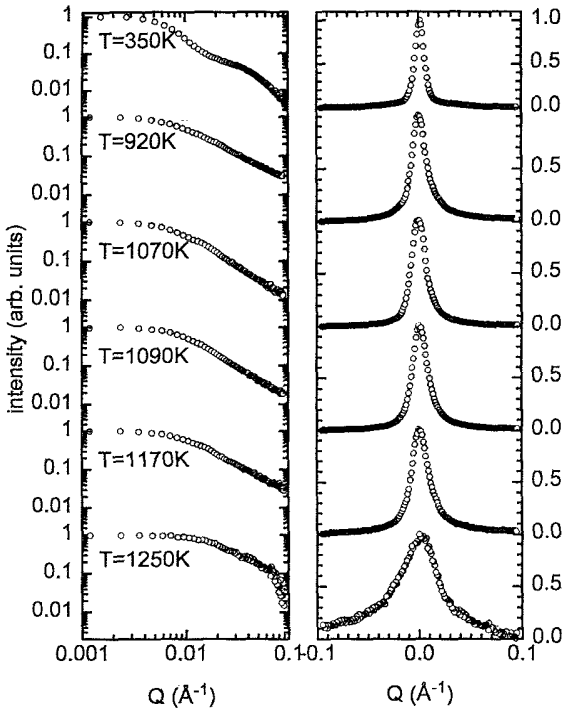

FIG. 10. Peak profiles of the specular (0,0) intensity along the [001] direction for antiphase scattering conditions ($E_{He}=17.8$ meV, $\vartheta_i=54.32°$) at different surface temperature. The profiles are plotted on a linear scale (right panel) and a double-logarithmic scale (left panel). The peak profiles (except for the upper curve at 350 K) can be described by a power-law line shape convoluted with the Gaussian instrument function. From a fit to the linear slope of the tails of the curves plotted in the double-logarithmic scale the power-law exponent can be determined for each temperature.

mining the power-law exponents from the experimental diffraction spectra is to determine the slope of the peak profile from a double-logarithmic representation of the data (Fig. 10). The results are summarized in Fig. 11. We find that the power-law exponent -1 is reached at a temperature of about 1095 K, providing a quantitative

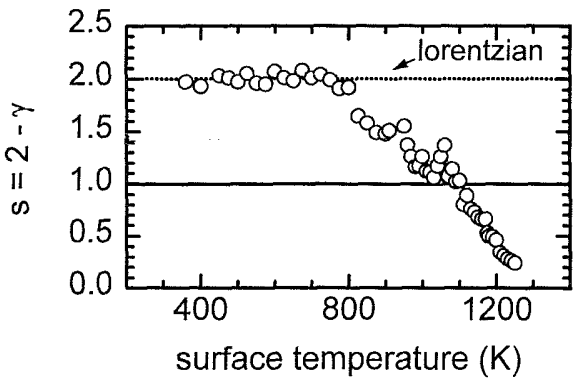

FIG. 11. Negative exponent s of the power-law line shape fitted to the tails of the antiphase (0,0) diffraction peaks in the double-logarithmic plot as shown in Fig. 10. $s=2-\gamma$ decreases with surface temperature and reaches a value of 1 at about 1095 K, which by definition is the surface roughening temperature T_R.

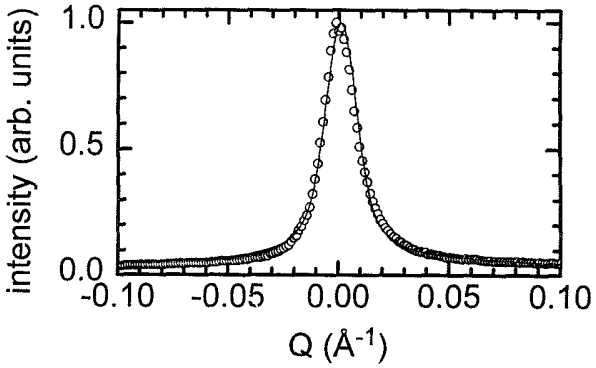

FIG. 12. Peak profile of the specular peak (0,0) for antiphase conditions ($E_{He}=17.8$ meV, $\vartheta_i=54.32°$) along the [001] direction at the roughening temperature $T_R=1095$ K. The line shape expected from theory is indicated by the solid line.

measure of the roughening temperature: $T_R=1095\pm20$ K. Note that this temperature is the same as that obtained from the FWHM of the diffraction peaks shown in Fig. 9. In Fig. 12, we have plotted the measured diffraction peak profile of the specular peak (0,0) under the antiphase condition at the roughening temperature $T_R=1095$ K together with the line shape given by the convolution of the power-law line shape (exponent -1) and the Gaussian instrument function.

It should be mentioned that the discussion of the roughening transition is based on time integrated intensities, including the coherent elastic as well as the phonon and diffuse elastic contributions. The theory, however, treats the purely elastic scattering only. The inelastic (multiphonon) scattering, which increases with the surface temperature, affects the correct determination of the roughening temperature. The peak profiles obtained from time integrated intensities exhibit a power-law line shape with exponent 1 at lower temperatures than the actual roughening temperature; i.e., they supply a lower limit for T_R.[54] Hence the separation between the deconstruction and roughening temperature would be even larger. In control experiments done during the present study, we did not find evidence for a significant difference between peak profiles with pure elastic intensity (using the TOF spectrometer) and those obtained with time integrated intensities. Hence, the determination of the roughening temperature seems not to be largely affected.

Finally, we point out that even at temperatures well below T_R the antiphase diffraction profiles are slowly changing with temperature (Figs. 9 and 11). This indicates that steps are formed on the Pt(110) surface already at lower surface temperature. This is not surprising and confirms that steps are involved in the deconstruction that precedes the surface roughening (see the discussion in Sec. III C).

The present results clearly support a separation between deconstruction and roughening opposite to the conclusions originally drawn from the x-ray diffraction experiments of Robinson, Vlieg, and Kern.[11] From the observation of a diffraction peak shift at the deconstruction temperature, these authors concluded that deconstruction and roughening take place at the same tempera-

ture. Villian and Vilfan[11(b)] suggested an alternative explanation of the x-ray diffraction experiments in which the steps formed above the transition are bound together in pairs. The imposition of paired steps leads necessarily to a phase transition model in the Ising-universality class due to the twofold degenerate ground state. This model forbids any height divergence and the surface is never rough. Villain and Vilfan suggest a step pair unbinding transition at higher temperatures $T_{c'} > T_c$ which eventually roughens the surface. Den Nijs,[23] however, suggests a transition with real roughening character but Ising criticality. In the framework of a four-state chiral clock step model, den Nijs demonstrates that for negligible chirality the reconstructed (1×2) fcc(110) surface deconstructs and roughens in one single transition that is characterized by Ising exponents. This transition has the character of an incommensurate melting transition, with respect to the reconstruction degrees of freedom, explaining the peak shift and the linear vanishing of it at T_c. Zero chirality, however, requires that step defects with a phase shift of $\frac{3}{2}\pi$ must also be present on the surface, but are rarely observed and are expected to be energetically unfavorable. More recently, Mazzeo *et al.*[28] demonstrated that a small diffraction peak shift in the initial phase of the transition might be obtained by a disordered flat phase with a random mixture of odd and even $(1\times n)$ configurations. In the simulation, the Ising disordering and the roughening are separated by about 30 K. At the roughening temperature they observe already a peak shift of 0.02 Å^{-1}. Assuming that the same shift would be characteristic for the roughening temperature of the Pt(110) surface, the x-ray measurements would in fact be consistent with the original Villian-Vilfan scenario of two successive phase transitions, Ising deconstruction and Kosterlitz-Thouless roughening.

IV. CONCLUSION

The structure of the (1×2) reconstructed clean Pt(110) surface and its changes with increasing surface temperature have been investigated using high-resolution thermal helium-atom scattering. The thermal behavior of the surface can be described by the following scenarios:

In the temperature range between 300 and 1000 K the surface is (1×2) reconstructed. The decrease of the diffraction peak intensities due to the increasing thermal vibrations of the surface atoms is described rather well by a conventional Debye-Waller factor. The effective Debye temperature of the Pt(110)-(1×2) surface is determined to be $\Theta_{D,\text{eff}} = 198$ K.

At temperatures around 1000 K surface defects (domain walls and steps) are generated in a significant quantity. This gives rise to a *deconstruction* of the surface at $T_c = 1025$ K. The resulting structure is a *disordered flat* (DOF) *phase* involving both types of defects, domain walls as well as steps. However, the precise microscopic structure of the DOF phase could not be quantified in detail. The deconstruction can be described by a 2D Ising model, in agreement with previous experimental work[11,26] and the theoretical prediction.[23]

At even higher temperatures more and more steps are generated spontaneously on the surface leading to a *roughening transition* of the surface. The surface-roughening transition can be described in terms of a Kosterlitz-Thouless transition; the critical temperature (roughening temperature) is determined to $T_R = 1095$ K.

The entire thermal behavior and all structural phase transitions involved are fully reversible.

[1]H. P. Bonzel, N. Freyer, and E. Preuss, Phys. Rev. Lett. **57**, 1024 (1986).
[2]H. Niehus, Surf. Sci. **20**, 407 (1984).
[3]E. C. Sowa, M. A. van Hove, and D. L. Adams, Surf. Sci. **199**, 174 (1988).
[4]E. Vlieg, I. K. Robinson, and K. Kern, Surf. Sci. **233**, 248 (1990).
[5]T. Gritsch, D. Coulman, R. J. Behm, and G. Ertl, Surf. Sci. **257**, 297 (1991).
[6]T. E. Jackman, J. A. Davies, D. P. Jackson, W. N. Unertl, and P. R. Norton, Surf. Sci. **170**, 389 (1982).
[7]H.-J. Brocksch and K. H. Bennemann, Surf. Sci. **161**, 321 (1985).
[8]S. M. Foiles, Surf. Sci. **191**, L779 (1987).
[9]P. Fery, W. Moritz, and D. Wolf, and Phys. Rev. B **38**, 7275 (1988).
[10]J. F. van der Veen, B. Pluis, and A. W. Denier van der Gon; in *Physics and Chemistry at Solid Surfaces VII* (Springer, Berlin 1988), p. 445.
[11](a) I. K. Robinson, E. Vlieg, and K. Kern, Phys. Rev. Lett. **63**, 2578 (1989); (b) I. Vilfan and J. Villain, *ibid.* **65**, 1830 (1990); (c) I. K. Robinson, E. Vlieg, and K. Kern, *ibid.* **65**, 1831 (1990).
[12]M. S. Daw and S. M. Foiles, Phys. Rev. Lett. **59**, 2756 (1987).
[13]J. Villain and I. Vilfan, Surf. Sci. **199**, 165 (1988).
[14]K. Rommelse and M. den Nijs, Phys. Rev. Lett. **59**, 2578 (1987).
[15]W. K. Burton, N. Carbrera, and F. C. Frank, Philos. Trans. R. Soc. London A **243**, 299 (1951).
[16]E. H. Conrad, Prog. Surf. Sci. **39**, 65 (1992).
[17]S. T. Chui and J. D. Weeks, Phys. Rev. B **14**, 4978 (1976).
[18]J. M. Kosterlitz and D. J. Thouless, J. Phys. C **6**, 1181 (1973).
[19]H. van Beijeren, I. Nolden, in *Structure and Dynamics of Surfaces II* (Springer, Berlin 1986), p. 259.
[20]G. H. Gilmer, Science **208**, 4442 (1980).
[21]M. den Nijs and K. Rommelse, Phys. Rev. B **40**, 4709 (1989).
[22]M. den Nijs, Phys. Rev. Lett. **64**, 435 (1990).
[23]M. den Nijs, Phys. Rev. B **46**, 10 386 (1992).
[24]M. den Nijs, Phys. Rev. Lett. **66**, 907 (1991).
[25]J. C. Campuzano and G. Jennings, R. F. Willis, Surf. Sci. **162**, 484 (1985).
[26]U. Korte and G. Meyer-Ehmsen, Surf. Sci. **271**, 616 (1992); **277**, 109 (1992).
[27]J. Sprösser, B. Salanon, and J. Lapujoulade, Europhys. Lett.

16, 283 (1991).
[28]G. Mazzeo, G. Jung, A. C. Levi, and E. Tosatti, Surf. Sci. **273**, 237 (1992).
[29]K. Kuhnke, Dissertation, Jül-Bericht 2490, KFA Jülich, 1991.
[30]C. Kittel, *Introduction to Solid State Physics* (Academic, London, 1961).
[31]G. Armand and J. R. Manson, Surf. Sci. **80**, 532 (1979).
[32]A. C. Levi and H. G. Suhl, Surf. Sci. **104**, 117 (1981).
[33]H.-D. Meyer, Surf. Sci. **104**, 117 (1981).
[34]N. Esbjerg and J. K. Nørskov, Phys. Rev. Lett. **45**, 807 (1980).
[35]H. Hoinkes, H. Nahr, and H. Wilsch, Surf. Sci. **33**, 516 (1972).
[36]G. Armand and J. R. Manson, Phys. Rev. B **37**, 4363 (1988).
[37]M. A. Krzyzowski, P. Zeppenfeld, and G. Comsa (unpublished).
[38]G. Garcia-Sanz and G. Armand, Solid State Commun. **28**, 79 (1978).
[39]J. Lapujoulade, J. Perreau, and A. Kara, Surf. Sci. **129**, 59 (1983).
[40]J. Lapujoulade, Y. Lejay, and G. Armand, Surf. Sci. **95**, 107 (1980).
[41]Note that the statistical error of ± 2 K does not include a possible error of the determination of the dead time of the detector. A potential error of about 10% in the dead time would lead to a systematic error in the Debye temperature of 15 K.
[42]V. Bortolani, V. Celli, A. Franchini, J. Idiodi, G. Santoro, K. Kern, B. Poelsema, and G. Comsa, Surf. Sci. **208**, 1 (1989).
[43]P. Zeppenfeld, K. Kern, R. David, and G. Comsa, Phys. Rev. Lett. **62**, 63 (1986).
[44]G. Armand and P. Zeppenfeld, Phys. Rev. B **40**, 5936 (1989).
[45]E. H. Conrad, L. R. Allen, D. L. Blanchard, and T. Engel, Surf. Sci. **198**, 207 (1988).
[46]P. Fenter and T. M. Lu, Surf. Sci. **154**, 15 (1985).
[47]The error is based on the standard deviation of the fits of Eq. (8) to the data in Fig. 7.
[48]J. C. Campuzano, M. S. Faster, G. Jennings, R. F. Willis, and W. Unertl, Phys. Rev. Lett. **54**, 2684 (1985).
[49]G. Blatter, Surf. Sci. **145**, 419 (1984).
[50]A. C. Levi, Surf. Sci. **137**, 385 (1984).
[51]F. Fabre, D. Grose, B. Salanon, and J. Lapujoulade, J. Phys. (Paris) **48**, 1017 (1987).
[52]E. H. Conrad, R. H. Aten, D. S. Kaufmann, L. R. Allen, T. Engel, M. den Nijs, and E. K. Riedel, J. Chem. Phys. **84**, 1015 (1986); **85**, 4756(E) (1986).
[53]A. Trayanov, A. C. Levi, and E. Tosatti, Europhys. Lett. **8**, 657 (1989).
[54]G. Barcco, C. Malò, C. J. Moses, and R. Tatarek, Surf. Sci. **287/288**, 871 (1993).